Forward four-wave mixing with defocusing nonlinearity

Shu Jia, Wenjie Wan, and Jason W. Fleischer*

Department of Electrical Engineering, Princeton University, Princeton, New Jersey 08544, USA
**Corresponding author: jasonf@princeton.edu*

Received December 14, 2006; revised March 5, 2007; accepted April 6, 2007;
posted April 17, 2007 (Doc. ID 78094); published June 5, 2007

We experimentally demonstrate degenerate, forward four-wave mixing effects in a self-defocusing photorefractive medium, in both one and two transverse dimensions. We observe the nonlinear evolution of new modes as a function of propagation distance, in both the near-field and far-field (Fourier space) regions.

OCIS codes: 190.4380, 190.4420.

Multiwave mixing, especially four-wave mixing (FWM), is a fundamental process in nonlinear optics. Nonlinearity couples the underlying modes, generating new sum and difference frequencies from the original waves. In the typical scenario, two pump waves interact with a signal wave, creating a daughter wave that is phase conjugated with the signal. While dispersion creates issues of phase matching, FWM has proved useful in such applications as real-time holography [1], supercontinuum generation [2], and soliton communication systems [3]. The most common configuration involves a self-focusing nonlinearity and a backward geometry, in which the initial pump beams counterpropagate to create a reflection grating. The focusing nonlinearity has the advantage of intensity concentration, but higher intensity can lead to other nonlinear effects, while the spatial (transverse) extent of interaction is limited by modulation instability. Furthermore, the backward geometry makes it difficult to cascade the wave mixing and follow the evolution of daughter waves. Here, we consider a forward (transmission) geometry, with all beams copropagating, in a self-defocusing medium. While both the configuration [4–7] and the nonlinearity [8,9] have been studied in FWM experiments, the evolution of cascaded modes has not been previously observed. We report such observations below, in both the near-field and the far-field (Fourier space) regions, in one and two transverse dimensions.

The beam system here is well described by the nonlinear Schrödinger equation,

$$i\frac{\partial\psi}{\partial z}+\frac{1}{2k_0}\nabla_\perp^2\psi+\Delta n(|\psi|^2)\psi=0, \qquad (1)$$

where ψ is the slowly varying amplitude of the optical field, $k_0=2\pi n_0/\lambda$ is the wavenumber in the material, and Δn is the index change induced by the light intensity. For a medium with a Kerr response, for which most theory is done, $\Delta n=(n_0 n_2\omega_0/2\pi)|\psi|^2$, where n_2 measures the strength of the nonlinearity ($n_2<0$ for defocusing). For the experiments considered here, a $2\text{ mm}\times 5\text{ mm}\times 10\text{ mm}$ strontium barium niobate (SBN) 75 crystal is used. In this case, the photorefractive nonlinearity $\Delta n=-(1/2)n_0^3 r_{33}E_{\text{app}}\bar{I}/(1+\bar{I})$, where $n_0=2.3$ is the base index of refraction, $r_{33}=1340$ pm/V is the appropriate electro-optic coefficient with respect to the applied field E_{app} and the crystalline axes, and the relative intensity $\bar{I}$ is the input intensity $|\psi|^2$ measured relative to a background (dark current) intensity [10,11]. A self-defocusing nonlinearity is created by applying a voltage bias of −125 V across the crystalline c axis and takes advantage of the photorefractive screening effect. In most cases, such as the experiments here, the use of defocusing nonlinearity minimizes the difference between Kerr and saturable systems [12].

The experimental setup is shown in Fig. 1. Light from a 532 nm laser is split by using Mach–Zehnder interferometers, creating an initial condition of interfering plane waves with k_x, $k_y=\{-k_1,k_{00},+k_1\}$. Since only a single frequency is used, the wave mixing within the photorefractive crystal is degenerate. Light exiting the crystal is then imaged into two CCD cameras, one for measuring the near field (x space), the other for recording the far field (k space). By using a rectangular crystal, rotation around the symmetry axis allows for the observation of wave-mixing effects after short (5 mm) and long (10 mm) propagation distances.

An example of symmetric FWM is shown in Fig. 2. Here, the initial condition is $k_{00}=0$, $k_1=\pi/D$ (i.e., an intensity profile $I(x)=I_0[1+b\cos(\pi x/D)]^2$), where

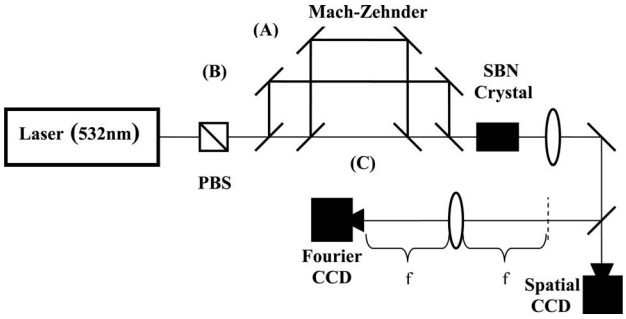

Fig. 1. Experimental setup. Light from a 532 nm laser is split by a polarizing beam splitter and sent to Mach–Zehnder interferometers (A), (B), together with background beam (C) forming the waveguide array on an SBN 75 crystal. The output face of the crystal is imaged into two CCD cameras: one for the near-field (position-space) intensity, the other for the far-field (Fourier space) pattern.

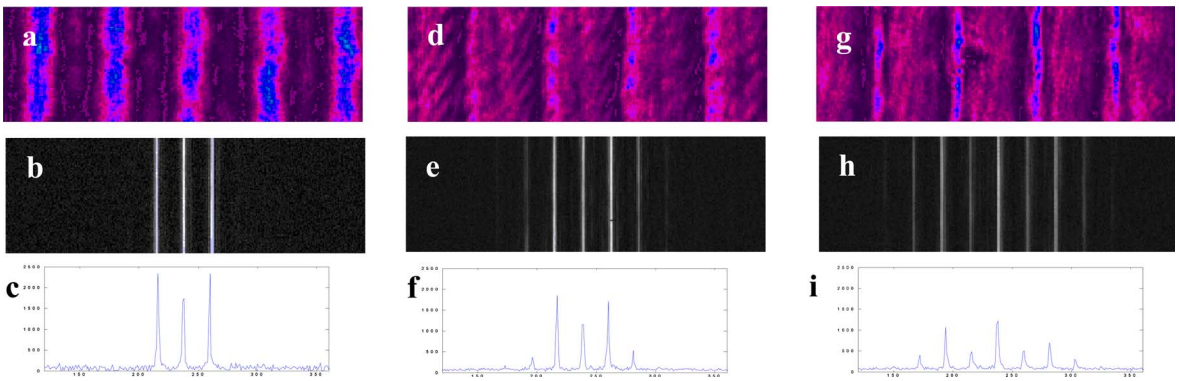

Fig. 2. (Color online) Experimental results of symmetric FWM versus propagation distance. Top row: near-field (position-space) intensity; middle row: Fourier picture; bottom row: Fourier cross sections. a–c, Linear input, where the spacing of the lattice is 80 μm and the intensity ratio of array to background beam is 3:1. c–e, Nonlinear output after 5 mm; g–i, Nonlinear output after 10 mm.

$D=80$ μm. While the spacing D and intensity ratio b are important parameters in determining the quantitative features of the output pattern, the general dynamics of the wave mixing are independent of the specific values chosen (provided $b\neq 0$). As shown in Figs. 2e and 2h, new spatial frequencies are generated as the light propagates. Mathematically, all higher harmonics are present immediately [the field amplitude ψ in Eq. (1) is the sum of all fields in the nonlinear medium], but physically it is seen that the higher momenta grow successively, with new modes appearing at equal k-space intervals as the light propagates and the daughter waves grow in intensity. Note that because one of the initial waves is at $k=0$, frequency differencing between waves causes spectral energy beating but does not generate new modes.

In the near field (position space), the generation of higher harmonics corresponds to an overall energy cascade to progressively smaller spatial scales. However, it is found that the original period D is maintained in this process; instead, the higher frequencies correspond to a narrowing of the intensity peaks (Figs. 2b and 2g). Despite the change from a sinusoidlike to a δ-like distribution, the maximum intensity of the peaks stays relatively constant. While focusing effects in self-defocusing media have been noted previously in the context of cross-phase modulation [13–15], the periodic conditions here suggest that a lattice interpretation is more appropriate; the initial beams effectively induce and self-populate a lattice, nonlinearly exciting higher-order Bloch modes with finer spatial scales [12]. The asymptotic behavior as this process cascades, however, has received little attention [16,17]. For example, the presence of a (spatial) frequency comb in k space runs counter to the intuition of an asymptotic state reducing to a flat, $k=0$ plane-wave characteristic of defocusing media, e.g., the limit of progressively widening Gaussians. One possibility is a (quasi)periodic behavior, such as breathing about a discrete spectral soliton [18,19], but this remains to be determined.

To study asymmetric FWM, we keep the $\cos(k_1 D)$ background but choose $k_{00}\neq 0$. Figure 3 shows the near-field and far-field (Fourier) patterns of the output, with tilted angles $k_{00}/k=0.625$ and 1.6 mrad. In these cases, the dynamical evolution is much more complex. In the near field, the initial spacing between the intensity peaks is no longer maintained, with a more intricate structure between them, and the focusing effect from cross-phase modulation is more clearly pronounced than in the symmetrical case. In the Fourier domain, the k-space peaks have a richer filling structure, with difference-frequency generation creating an inverse cascade to larger scales. For rational initial ratios, there is ultimately the smallest spacing between k-space peaks; for irrational initial ratios, this is not the case, and dense filling fractions are possible.

The geometry dependence of FWM is even more significant in two dimensions. Figure 4 shows the simple case of four symmetrically interfering plane waves and a background beam, with an intensity distribution $I(x,y)=I_0[1+b(\cos(\pi x/D)+\cos(\pi y/D))]^2$. At the input face, the interference pattern consists of a square array of circular Gaussians in the real space

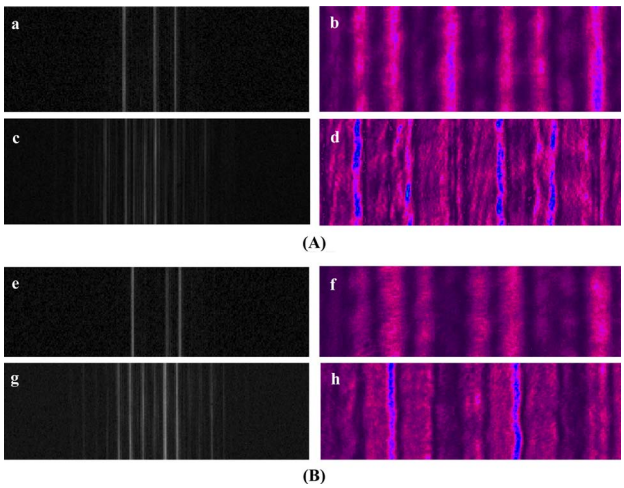

Fig. 3. (Color online) Asymmetric FWM using angled background beam (A) tilted by 0.625 mrad, (B) tilted by 1.6 mrad. Left column: Fourier picture; right column: near-field (position-space) intensity. a, b, e, f, Linear input, where the spacing of the lattice is 80 μm and the intensity ratio of array to background beam is 3:1; c, d, g, h, Nonlinear output after 10 mm.

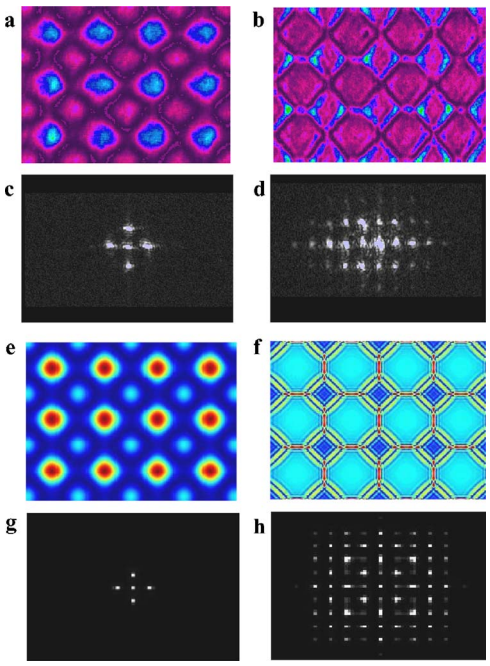

Fig. 4. (Color online) Two-dimensional degenerate FWM with defocusing nonlinearity. a–d, Experimental results. e–h, Simulation results. Left column: linear input, where the period of the arrays is 80 μm. Intensity ratio of array to background is 3:1. Right column: nonlinear output. a, b, e, f, Near-field (position-space) intensity. c, d, g, h, Far-field (Fourier) picture.

and a diamond of five spots in the Fourier space. After nonlinear propagation, the higher intensity areas in real space are stretched out to form squarelike patterns. (The asymmetry in both positions and the Fourier space is due to the underlying anisotropy of the SBN crystal.) Computer simulations, also shown in Fig. 4, reveal that reflections create a series of nested squares during propagation, each with well-defined straight-line boundaries. Effectively, the initially circular Gaussians defocus and interact, canceling their curvature due to superposition; the resulting straight-line sources then defocus themselves, interacting *ad infinitum*. Similar curvature cancellation and nonlinear propagation have been seen in collisions of dispersive spatial shock waves [20]. Indeed, the geometry can be considered an array of high-intensity humps that shock the ambient background.

In summary, we have demonstrated degenerate, forward four-wave mixing processes using self-defocusing nonlinearity, in both one and two transverse dimensions. The generation of new modes depended sensitively on the crossing angle and intensity ratio of the incoming beams. In two dimensions, wavefront and array geometry contributed significantly to wave mixing and interaction. In all cases, the dynamics were characterized by spectral beating between the parent and daughter waves. Cross-phase focussing effects were seen, and several generations of daughter waves were observed in both the near-field and far-field (Fourier) spaces. The asymptotic state, however, is beyond the range of current experiments and remains an open question.

This work was supported by the National Science Foundation (NSF) and the U.S. Air Force Office of Scientific Research (AFOSR).

References

1. A. Yariv and D. M. Pepper, Opt. Lett. **1**, 16 (1977).
2. R. R. Alfano and S. L. Shapiro, Phys. Rev. Lett. **24**, 584 (1970).
3. M. J. Ablowitz, G. Biondini, S. Chakravarty, R. B. Jenkins, and J. R. Sauer, J. Opt. Soc. Am. B **14**, 1788 (1997).
4. V. Kondilenko, S. Odoulov, and M. Soskin, Ferroelectr., Lett. Sect. **1**, 19 (1983).
5. A. Khyzniak, V. Kondilenko, Y. Kucherov, S. Lesnik, S. Odoulov, and M. Soskin, J. Opt. Soc. Am. A **1**, 169 (1984).
6. B. Fischer, J. O. White, M. Cronin-Golomb, and A. Yariv, Opt. Lett. **11**, 239 (1986).
7. J. Takacs, H. C. Ellin, and L. Solymar, Opt. Commun. **93**, 223 (1992).
8. I. V. Tomov and P. M. Rentzepis, Appl. Phys. Lett. **64**, 1 (1994).
9. O. Werner, B. Fischer, and A. Lewis, Opt. Lett. **17**, 241 (1992).
10. M. Segev, B. Crosignani, P. Diporto, A. Yariv, G. Duree, G. Salamo, and E. Sharp, Opt. Lett. **19**, 1296 (1994).
11. D. N. Christodoulides and M. I. Carvalho, J. Opt. Soc. Am. B **12**, 1628 (1995).
12. J. W. Fleischer, G. Bartal, O. Cohen, T. Schwartz, O. Manela, B. Freedman, M. Segev, H. Buljan, and N. K. Efremidis, Opt. Express **13**, 1780 (2005).
13. G. P. Agrawal, Phys. Rev. Lett. **59**, 880 (1987).
14. J. M. Hickmann, A. S. L. Gomes, and C. B. Dearaujo, Phys. Rev. Lett. **68**, 3547 (1992).
15. A. J. Stentz, M. Kauranen, J. J. Maki, G. P. Agrawal, and R. W. Boyd, Opt. Lett. **17**, 19 (1992).
16. N. Korneev, A. Apolinar-Iribe, and J. J. Sanchez-Mondragon, J. Opt. Soc. Am. B **16**, 580 (1999).
17. N. Korneev and F. Marroquin, J. Opt. Soc. Am. B **24**, 84 (2007).
18. S. Flach, M. V. Ivanchenko, and O. I. Kanakov, Phys. Rev. Lett. **95**, 064102 (2005).
19. A. V. Gorbach and D. V. Skryabin, Opt. Lett. **31**, 3309 (2006).
20. W. Wan, S. Jia, and J. W. Fleischer, Nat. Phys. **3**, 46 (2007).